

DAMO: DECODING BY ACCUMULATING ACTIVATIONS MOMENTUM FOR MITIGATING HALLUCINATIONS IN VISION-LANGUAGE MODELS

Anonymous authors

Paper under double-blind review

ABSTRACT

Large Vision-Language Models (LVLMs) exhibit significant potential in multimodal tasks but often struggle with hallucinations—responses that are plausible yet visually ungrounded. In this work, we investigate the layer-wise prediction tendencies of LVLMs and conduct an in-depth analysis of their decoding mechanism. We observe that LVLMs tend to “overthink” during the final stages of decoding, making significant prediction shifts in the last few layers often favoring incorrect results, which leads to a surge in hallucinative outputs. Leveraging this localized pattern, we propose a novel decoding strategy inspired by the momentum analogy used in gradient descent-based optimizers. Our method enforces decoding consistency across layers in an adaptive manner during forward passes—an under-explored approach in existing works. This strategy significantly improves the reliability and performance of LVLMs in various multimodal tasks, while introducing only negligible efficiency overhead.

1 INTRODUCTION

The recent advancement in model architecture and training methodologies has led to unprecedented development and wide adoption of Large Vision-Language Models (LVLMs) (Devlin, 2018; Chen et al., 2019; Liu et al., 2024c; Zhou et al., 2023a; Ye et al., 2023b). Through bridging the gap between visual and textual modalities, they offer a viable and promising solution for various multimodal tasks such as visual question answering and image captioning (Liu et al., 2024d; Ye et al., 2023a; Zhu et al., 2023b; Li et al., 2023b; Lee et al., 2024). Despite their success, LVLMs continue to struggle with hallucinations (Liu et al., 2023a; Yin et al., 2023), a phenomenon where they tend to generate syntactically plausible yet visually ungrounded responses (see Fig. 1a). This intractable challenge significantly undermines users’ trust in their output, thereby hindering their broader application in real-world scenarios (Chen et al., 2024b; Hu et al., 2023; Liu et al., 2023b).

Several studies have delved into the mechanisms behind hallucinations, attributing them to factors such as over-reliance on statistical pre-training biases (Agarwal et al., 2020; Agrawal et al., 2016), language priors, and attention deficiency (An et al., 2024). All these proposed conjectures suggest that the inherent neglect of modality information integrated at later stages can lead to inaccurate outputs. Additionally, indiscriminate associative reasoning on linguistic and visual data can cause hallucinated responses to gradually dominate the decoding distribution. Thus they leverage knowledge editing methods (De Cao et al., 2021; Meng et al., 2022) to inject new answers or knowledge into foundation models and to erase hallucination on mis-answered samples. The existing methods edit knowledge of LVLMs by either fine-tuning specific memory parameters or maintaining an external memory of updated knowledge facts. Despite these efforts, we propose a critical doubt remains unresolved: *Does LVLMs really don’t know ground-truth answers for solving those hallucinated problems?* This suspicion is originated from following observation that LVLMs generally can decode the desired outputs at early layers but later they turn to focus on other unrelated contents.

To answer this question, we analyze the layer-wise prediction tendencies of LVLMs and summarize the patterns of hallucination progressing accordingly. Specifically, we leverage a vanilla MiniGPT-4 Zhu et al. (2023c) and manually collect an evaluation dataset on visual question answering task

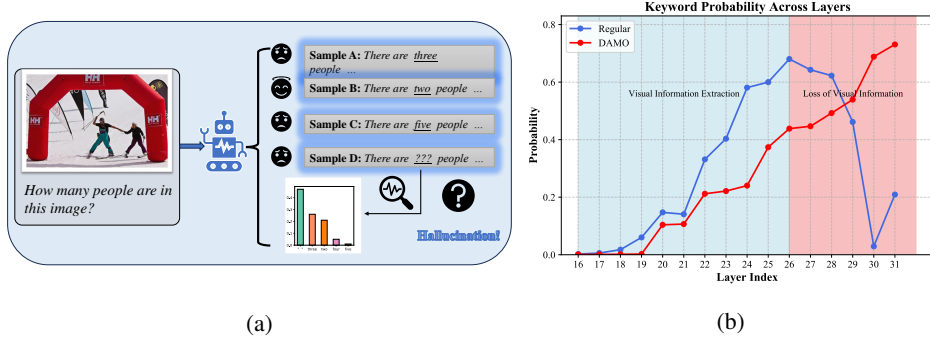


Figure 1: (a) Hallucination example: the model is asked “How many people are in this image?” for an image of two people skiing. And the analysis of probability distribution for key token. (b) Probability of predicting the token ‘two’ across layers. The blue curve shows Regular decoding, while the red shows the effect of DAMO. The shaded area marks the stages of *Visual Information Extraction* and *Loss of Visual Information*.

from COCO val2014 Lin et al. (2014). Motivated by the idea of *early exit* (Teerapittayanon et al., 2016; Elbayad et al., 2019; Schuster et al., 2022), we decode the immature hidden states exited by LVLMs in advance and pay attention to confidence variations of the ground-truth token across layers. A qualitative illustration of this phenomenon is shown in Fig. 1b: The decoding probability of the ground-truth answer, ‘two’, steadily increases across the early layers and then dominates the decoding distribution, revealing that LVLMs internally owns the capability to extract the fine-grained visual semantics. However, its decoding tendency drastically deviates at the later layers and token ‘two’ is not the first choice anymore at the last layer. Based on this observation, we hypothesize that the hallucinations within LVLMs manifest as **localized surges** at the later layers, which in turn suppresses the pre-existing and visual related information in the decoding distribution, ultimately leading to visually ungrounded responses.

To address these concerns and improve the truthfulness of LVLMs, we propose a novel decoding method, **Decoding by Accumulating Activations MOmentum (DAMO)**. Specifically, DAMO accumulates a momentum by aggregating the activations layer-by-layer and uses this momentum, which contains the historical updating trends, to correct hidden states at the later layers of LVLMs. This approach amplifies visual semantics consistently extracted throughout the inference while reducing hallucination biases that are intensively introduced at the later layers. This idea is built upon two foundations: ❶ In gradient descent, momentum has been widely proven to an effective acceleration technique by accumulating persistent updates towards low-curvature directions, driving the model closer to the global optimum (Sutskever et al., 2013; Polyak, 1964). ❷ Ahn et al., 2024 have demonstrated that a transformer can implement preconditioned gradient descent, and that the forward computation process of a L -layer transformer is conditionally equivalent to L steps of gradient descent. Therefore, implementing “momentum” in the forward computation of transformers to counteract the localized and intense emergence of hallucinations is an intuitive and expectedly effective approach. Fig. 1b shows that DAMO successfully reduces the hallucinations that occur during the inference of the vanilla MiniGPT-4.

Experiments on MME and POPE datasets across various LVLMs demonstrate that DAMO significantly mitigates hallucinations, resulting in more visually grounded and accurate predictions. When applied to mPLUG-Owl2 Ye et al. (2023b) without any additional training, DAMO achieved a remarkable 100-point improvement over regular decoding on the MME dataset, outperforming all other baseline methods. Building on this success we further extended DAMO to LLMs, where is also delivered strong results on benchmarks such as TruthfulQA Lin et al. (2021), FACTOR Muhlgay et al. (2023), and GSM8K Cobbe et al. (2021), indicating that DAMO possesses notable transferability across different tasks and model types. The contributions of this paper are summarized as follows:

- We identify that hallucinations in Vision-Language Models (LVLMs) primarily occur during the inference process and are driven by localized surges in the later layers, which suppress visual information.

- We introduce Decoding by Accumulating Activations Momentum (DAMO), a novel approach that reduces hallucinations by accumulating activation momentum, significantly improving visual grounding in LVLMs across multiple benchmarks.

2 RELATED WORK

Large Vision-Language Models The evolution of Vision-Language Models (LVLMs) has progressed from BERT-based models (Devlin, 2018; Lu et al., 2019; Tan & Bansal, 2019; Chen et al., 2019) to those integrated with Large Language Models (LLMs) (Liu et al., 2023c; Zhu et al., 2023c; Zhou et al., 2023a; Ye et al., 2023b), which have significantly improved their capabilities. Early models like ViLBERT Lu et al. (2019), LXMERT Tan & Bansal (2019), and UNITER Chen et al. (2019) effectively merged visual and textual features using BERT-style architectures. The introduction of LLMs enabled LVLMs such as CLIP Radford et al. (2021) and ALIGN Jia et al. (2021), which significantly enhanced adaptability and performance through end-to-end training. Recent works like LLaVA (Liu et al., 2023c; 2024b) and InstructBLIP Dai et al. (2023) further refined these models using visual instruction fine-tuning, demonstrating adaptability across diverse vision-language tasks and showcasing a growing trend toward task-specific approaches.

Hallucinations in LVLMs In Large Language Models (LLMs), hallucinations have been extensively studied (Ji et al., 2023; Yao et al., 2023; Zhang et al., 2023b;a; Liu et al., 2024a; Xu et al., 2024), particularly in contexts where generated text diverges from the input or factual reality. In LVLMs, hallucinations present additional challenges due to the alignment between visual and textual data (Biten et al., 2022; Li et al., 2023c; Wang et al., 2024), which increases the potential for hallucinations. This issue is particularly prevalent in tasks such as image captioning and visual question answering (Liu et al., 2023a; Yin et al., 2023; Zhou et al., 2023b; Zhu et al., 2024a; Gunjal et al., 2024), where maintaining coherence between modalities is critical.

Addressing Hallucinations in LVLMs Some researches (Gunjal et al., 2024; Wang et al., 2024) have attempted to mitigate hallucinations through fine-tune models. However, this approach can be resource-sensitive, leading to increased computational costs, while also risking a decline in performance on other tasks and limiting the model’s overall versatility. Additionally, there are also some approaches (Zeng et al., 2021; Kim et al., 2023; Zhou et al., 2023b) trying to enhance alignment between visual and text modalities to address hallucinations.

At the same time, DoLA Chuang et al. (2023) has been proposed to address hallucination issues in LLMs through contrasting decoding, achieving promising results without the need for additional training. Subsequently, contrasting decoding was applied in LVLMs to address hallucination issues. VCD (Visual Contrastive Decoding) Leng et al. (2024) is a training-free method designed to mitigate object hallucinations in LVLMs, contrasting output distributions from original and distorted visual inputs to reduce reliance on statistical bias and unimodal priors. HIO (Hallucination-Induced Optimization) Chen et al. (2024a) addresses hallucinations in LVLMs by amplifying the contrast between hallucinatory and targeted tokens using a fine-tuned Contrary Bradley-Terry Model. IBD (Image-Biased Decoding) Zhu et al. (2024b) mitigates hallucinations in LVLMs by contrasting predictions from a standard LVLm with those from an image-biased LVLm, amplifying image-related information and reducing over-reliance on text. The common issue with these methods is that they only correct the next token prediction through logits contrasting at the final layer, without attempting to identify and address hallucinations in the hidden states during the inference process. In addition, OPERA Huang et al. (2024) mitigates hallucination by reducing reliance on summary tokens during decoding and adjusting token selection based on previously generated tokens.

3 METHOD

We first introduce the decoding process in LVLMs to provide some preliminaries. Next, we elaborate our motivation to transfer the idea of momentum into LVLm decoding by an intuitive example. Finally, we propose a novel, seamlessly integrated decoding method called DAMO, which accumulates the raw activation updates into the momentum layer by layer to correct the hidden states’ updating direction, effectively smoothing the update process and mitigating hallucinations.

3.1 DECODING IN VISION-LANGUAGE MODELS

Given an input representation h_t^0 at time step t , the standard decoding process of a N -layer LVLM is outlined as follows (Liu et al., 2024c; Zhu et al., 2023a; Li et al., 2023a):

$$\begin{cases} h_t^{j+1} = f_j(h_t^j) + h_t^j, & j = 0, \dots, N-1, \\ p(x_{t+1}|x_{:t}) = \text{softmax}(\phi(h_t^N)), \end{cases} \quad (1)$$

where $f_j(\cdot)$ refers to the j -th transformer layer, and h_t^j denotes the hidden states at layer j at time step t . $f_j(h_t^j)$ represents the activation output by layer j , which is the sum of the activations produced by both the MLP and the self-attention modules at the current layer. $\phi(\cdot)$ represents the language head that predicts the next-token probability over the entire vocabulary. Although $\phi(\cdot)$ is only trained to transform the final-layer activation (i.e., h_t^N) into the next-token distribution, several studies (Teerapittayanon et al., 2016; Elbayad et al., 2019; Schuster et al., 2022) have demonstrated that applying the language head directly to intermediate activations exited from earlier layers can also produce meaningful distributions, reflecting prediction tendencies of LVLMs. We formally describe *early exit* as follows:

$$p_j(x_{t+1}|x_{:t}) = \text{softmax}(\phi(h_t^j)), \quad j = 1, \dots, N-1. \quad (2)$$

Here, h_t^j refers to the intermediate activation exited by layer j at time step t . In Section 3.2, we utilize this technique to illustrate our motivation.

3.2 MOTIVATION

In Visual Question Answering (VQA), LVLMs take an image and a related question as input, producing an answer based on visual cues. We conducted a preliminary experiment on a small-scale, self-constructed dataset to explore hallucinations in LVLMs. The dataset, derived from randomly selected images from COCO val2014 Lin et al. (2014), included questions focused on quantifiable attributes such as color, number, and direction. We identified 100 instances exhibiting hallucinations and analyzed the probability distribution of key words (e.g., ‘two’ in Figure 1b) across the model’s layers during inference.

Our findings revealed that 75% of the samples shared a consistent issue: while LVLMs are adept at extracting visual information from images, hallucinations frequently emerge in the later layers of the inference process. This analysis highlighted two key insights: ① LVLMs are already proficient in capturing detailed visual information, so further intensifying image-text fusion is unnecessary. ② Hallucinations primarily occur during later inference stages, so we only need to correct hallucinations at these stages of the inference process.

Motivated by this, we propose DAMO that refines activations by leveraging earlier layer information, helping to preserve visual context and reduce hallucinations, ultimately improving prediction accuracy.

3.3 DECODING BY ACCUMULATING ACTIVATION MOMENTUM

Momentum in Gradient-based Optimization Momentum, a popular technique in gradient-based optimization, has been proven to be fairly effective for providing better convergence rate (Polyak, 1964). The idea of this method is to preserve the historical updating trends from previous steps in the momentum and use this value to correct the update direction of the current step. Specifically, the model parameters θ_t at the current step t are obtained according to the following formula:

$$\begin{cases} v_t = \beta v_{t-1} + (1 - \beta) \nabla L(\theta_{t-1}), \\ \theta_t = \theta_{t-1} - \eta v_t. \end{cases} \quad (3)$$

Here, η represents the learning rate, and $\nabla L(\theta_{t-1})$ denotes the gradient w.r.t. the training objective. The term v_t accumulates past gradients, serving as the *real updates* at the current step, while β is the trade-off coefficient balancing historical and current information. This momentum-based approach is particularly effective in training deep neural networks, as it smooths the optimization trajectory, improving both stability and convergence speed (Sutskever et al., 2013).

Starting Layer	Existence	Count	Position	Color	Posters	Celebrity	Scene	Landmark	Artwork	OCR	Total
Vanilla Decoding	190.00	160.00	138.33	165.00	141.50	135.88	156.25	161.25	118.50	125.00	1491.71
0-th	185.00	115.00	123.33	153.33	78.57	90.29	139.75	107.00	105.75	132.5	1230.53
10-th	185.00	115.00	118.33	168.33	81.63	89.71	136.00	102.75	108.00	110.00	1214.76
16-th	195.00	145.00	138.33	165.00	143.54	136.76	157.75	166.00	118.50	140.00	1505.89
18-th	190.00	145.00	133.33	160.00	144.56	136.47	159.75	167.75	121.50	130.00	1488.36
20-th	195.00	150.00	133.33	165.00	142.52	134.12	157.00	165.25	115.75	132.50	1490.47
22-th	190.00	150.00	143.33	165.00	144.56	134.41	156.25	167.5	118.25	132.50	1501.80
24-th	195.00	153.33	148.33	165.00	142.52	134.71	157.00	163.75	116.25	132.50	1508.39

Table 1: Using LLaVA1.5 as the foundation model, the performance of **Activation Momentum** with different refinement starting layer on the MME dataset. Each column refers to a hallucination category and the best results in each column are marked with **bold**.

Activation Momentum in Vision-Language Models Inspired by traditional momentum, we introduce the *Activation Momentum (AM)* in LVLMs, expecting to transfer its beneficial properties – guiding the change of hidden states toward a consistent and smooth update direction while preventing abrupt or localized deviations from historical updates. Specifically, given the hidden state h_t^j at layer j at time step t , the j -th transformer layer $f_j(\cdot)$ can produce the raw activation $\nabla h_t^{j+1} = f_j(h_t^j)$. In vanilla decoding process, the next-layer hidden state is obtained directly by $h_t^{j+1} = h_t^j + \nabla h_t^{j+1}$. To accumulate the previous activation status used to correct later layers, our proposed AM first integrates ∇h_t^{j+1} into the momentum term v_t^j . The momentum variable is formally defined as:

$$v_t^{j+1} = \beta v_t^j + (1 - \beta) \nabla h_t^{j+1}, \quad (4)$$

where β , similar to its role in gradient descent, is the trade-off coefficient balancing historical and current information. And the term v_t^{j+1} represents the momentum after incorporating the raw activation produced at the current step, which actually serves as the refined activation. Therefore, the revised updating process of hidden states is shown as below:

$$h_t^{j+1} = h_t^j + v_t^{j+1}, \quad (5)$$

where h_t^{j+1} can partially reflect the update trends of the previous layers and will then serve as the input to the subsequent layer.

3.4 MECHANISM OF ADAPTIVE ACTIVATION REFINEMENT

AM represents a naive implementation of momentum-based decoding in LVLMs. However, unlike its use in optimization, we argue that while it is essential to maintain the momentum value (Equ. 4) all the time in order to preserve more historical information, Equ. 5 does not need to be applied across all layers. This is because hallucinations primarily emerge in the later layers so continuously refining the raw activations may suppress valuable updates encoding rich visual semantics generated by certain early layers.

To validate our proposition, we conduct a preliminary experiment on the MME dataset (Fu et al., 2023), a comprehensive benchmark to measure the ability of LVLMs in various aspects. The results shown in Table. 1 demonstrate that: ① Starting activation refinement too early (at layer 0 or 10) significantly impairs the visual reasoning ability of LVLMs. ② Varying the starting layer for refinement can enhance different model capabilities (e.g., layer 16 excels in OCR tasks, while layer 24 improves positional perception). These observations suggest that activation refinement should begin in the later layers, and a fixed starting layer is insufficient to achieve comprehensive improvements across various key abilities of LVLMs.

Thus, we propose the *mechanism of adaptive activation refinement*, which also leverages the idea of momentum and adaptively determines, during forward computation, whether the model has reached the **hallucination surge** and selects the appropriate refinement starting layer. This mechanism, together with AM, constitutes our complete approach, **D**ecoding by **A**ccumulating **A**ctivations **M**omentum (DAMO). For simplicity of notations, we denote the early exit distribution $p_j(x_{t+1}|x_{:t})$ at layer j (from Equ. 2) as P^j . We focus on the update direction of the early exit distribution, main-

taining momentum $\nabla \hat{P}^j$ to accumulate the update trends of the previous layers:

$$\begin{cases} \nabla P^j = P^j - P^{j-1}, \\ \nabla \hat{P}^j = \alpha \nabla \hat{P}^{j-1} + (1 - \alpha) \nabla P^j, \end{cases} \quad (6)$$

where ∇P^j denotes the relative change of the early exit distribution caused by layer j , reflecting the current prediction tendencies of LVLMS. $\nabla \hat{P}^j$ is the momentum variable, preserving historical prediction trends of previous layers. Intuitively, if ∇P^j diverges significantly from the momentum variable $\nabla \hat{P}^j$, it indicates a notable deviation from the original trend, potentially signaling the onset of hallucination patterns. Based on this hypothesis, we use the cosine similarity between ∇P^j and $\nabla \hat{P}^j$ as the criterion for triggering activation refinement. Building on this hypothesis, we use the cosine similarity between ∇P^j and $\nabla \hat{P}^j$ as the criterion for triggering activation refinement. Specifically, if the similarity falls below a predetermined threshold τ , activation refinement is initiated and continues until the final layer.

3.5 COEFFICIENT ADJUSTMENT FOR NOISE-RESISTANT MOMENTUM

After we have reached the **hallucination surge**, keeping the trade-off coefficient β (from Equ. 4) fixed leads to several issues: The hallucinated activations produced by the later layers will be incorporated into the activation momentum v_t^j , acting as noise and gradually diluting the correct historical information it contains. To address this, we set the initial value of β to β_1 and change its value according to the following rules:

$$\beta = \begin{cases} \beta_2 & \text{if } \text{Cosine}(\nabla P^j, \nabla \hat{P}^j) < \tau \\ \beta_1 & \text{if } \text{Cosine}(\nabla P^j, \nabla \hat{P}^j) \geq \tau \end{cases} \quad (7)$$

Here we must ensure that $\beta_1 < \beta_2$. Transitioning from β_1 to β_2 means that the onset of a hallucination surge, accompanied by significant changes in prediction tendencies. Consequently, it becomes necessary to preserve more historical information (set a higher value for β , i.e. β_2), enhancing v_t^j , the momentum term’s resistance to these hallucinatory elements.

4 EXPERIMENTS

In experiments, we first introduced the datasets, models, and baselines in the Setup section, followed by a detailed presentation of the Results. We evaluated our DAMO method on the comprehensive hallucination dataset MME and examined object hallucination using the SEEM-annotated MSCOCO and A-OKVQA datasets from POPE. To assess robustness, we tested on the generalized dataset LLaVA-Bench. Additionally, we evaluated the adaptive activation refinement for starting layer selection and adaptive coefficient adjustment. Finally, we applied our DAMO to LLMs to assess its transferability to mitigate hallucinations.

4.1 SETUP

Datasets We evaluate our proposed method using four datasets designed to assess hallucination issues in large Vision-Language Models (LVLMS). MME Fu et al. (2023) offers a comprehensive benchmark featuring 14 tasks categorized into perception and cognition. POPE (Polling-based Object Probing Evaluation) Li et al. (2023c) is a scalable framework for detecting object hallucinations in LVLMS, utilizing SEEM-annotated datasets from MSCOCO Lin et al. (2014) and A-OKVQA Schwenk et al. (2022). LLaVA-Bench, a generalized dataset, comprising 24 diverse images and 60 questions across categories like simple QA, detailed descriptions, and complex reasoning, is used to further evaluate the model’s generalization and robustness.

Models Numerous high-performing LVLMS have emerged recently. For our evaluation, we selected three models: LLaVA1.5 Liu et al. (2023c), INF-MLLM1 Zhou et al. (2023a), and mPLUG-Owl2 Ye et al. (2023b), each demonstrating strong performance on established benchmarks. Notably, all these LVLMS are equipped with a 7B Large Language Models (LLMs).

Baselines We compare our method with four baselines. Regular responses are generated using the original LVLMS. Visual Contrastive Decoding (VCD) Leng et al. (2024) mitigates object hallucinations by contrasting output distributions from original and distorted visual inputs. DOLA Chuang

et al. (2023) is transferred to LVLMs, with a fixed mature layer index at 32 and multiple candidate premature layer indices (“0, 2, 4, 6, 8, 10, 12, 14”) to fine-grain the model’s internal decision-making process. For OPERA Huang et al. (2024), due to the computational resource limitations, we set *num.beams* to 4, while keeping all other settings consistent with its official configuration. To ensure fairness, we set the temperature to 0 for all comparisons.

Hyperparameters Setting We have provided all the hyperparameters used in our experiments, including τ , β_1 , β_2 and α , which can be found in the Appendix. Additionally, we tested the model’s sensitivity to these hyperparameters, with detailed experimental results also available in the Appendix. The experimental results confirm that our hyperparameter selection is optimal.

4.2 RESULTS

Evaluation on Comprehensive Hallucination Dataset

▷ *Implementation* We adopted the MME benchmark to evaluate DAMO across 3 models and reported results in the perception category, which contains 10 tasks, following the settings used in other hallucination studies.

▷ *Q: Whether our DAMO outperforms other decoding methods on the comprehensive dataset?* Yes, as shown in Table 2, we present the experimental results of various decoding methods on the MME dataset. Notably, DAMO almost outperformed other decoding strategies across all models, achieving a total scores of 1515.89, 1520.74 and 1437.46 on LLaVA1.5, INF-MLLM1 and mPLUG-Owl2, respectively. Specifically, on the mPLUG-Owl2 model, DAMO surpassed the VCD method by 38.91 points. Moreover, in the “Celebrity” task, it achieved the highest score of 164.41 among all methods. Additionally, DOLA demonstrated no performance enhancement on the INF-MLLM1 model, suggesting that directly transferring DOLA to LVMs may not guarantee performance improvements.

▷ *Q: Does our DAMO also have relatively low memory consumption?* Yes, our DAMO also exhibits relatively low memory consumption. As shown in the last column of Table 2, the memory consumption of DAMO is nearly identical to that of Regular. In contrast, VCD requires two forward passes to contrast output distributions from original and distorted visual inputs, necessitating the storage of logits from both passes. DOLA also needs to retain logits from intermediate premature layers, while OPERA utilizes beam search, resulting in significantly higher memory consumption—up to 50GB on the INF-MLLM1 model. In summary, DAMO does not require storing any intermediate logits, as we continuously use momentum for modifications, which contributes to its efficiency in memory usage.

Model	Decoding	Existence	Count	Position	Color	Posters	Celebrity	Scene	Landmark	Artwork	OCR	Total	Memory
LLaVA1.5	Regular	190.00	160.00	138.33	165.00	141.50	135.88	156.25	161.25	118.50	125.00	1491.71	14.6GB
	VCD	188.33	140.00	133.33	155.00	137.76	139.12	153.25	166.00	120.75	125.00	1458.54	15.6GB
	DOLA	190.00	158.33	143.33	165.00	139.46	133.24	157.75	160.50	119.50	125.00	1492.11	15.1GB
	OPERA	195.00	158.33	148.33	175.00	142.52	131.18	157.00	161.50	117.00	132.50	1518.36	22.5GB
	DAMO	195.00	150.00	143.33	165.00	144.56	135.00	157.00	166.00	120.00	140.00	1515.89	14.6GB
INF-MLLM1	Regular	195.00	150.00	151.67	160.00	150.00	140.29	157.75	155.50	122.50	110.00	1492.71	17.6GB
	VCD	190.00	138.33	160.00	160.00	142.52	135.59	157.00	153.50	113.25	105.00	1455.19	18.6GB
	DOLA	195.00	150.00	151.67	160.00	150.00	140.29	157.75	155.50	122.50	110.00	1492.71	18.2GB
	OPERA	195.00	155.00	151.67	160.00	149.32	139.41	156.25	154.00	122.50	110.00	1493.15	48.8GB
	DAMO	195.00	150.00	158.33	165.00	148.64	146.76	156.25	154.75	128.50	117.50	1520.74	17.6GB
mPLUG-Owl2	Regular	180.00	145.00	73.33	136.67	136.73	141.18	157.25	137.75	127.25	102.50	1337.66	16.1GB
	VCD	185.00	155.00	63.33	148.33	142.86	158.53	154.00	141.00	133.00	117.50	1398.55	16.4GB
	DOLA	190.00	160.00	70.00	150.00	145.92	159.12	160.50	151.25	130.25	110.00	1427.04	16.2GB
	OPERA	190.00	160.00	70.00	150.00	145.92	160.88	160.50	150.50	131.00	110.00	1428.80	24.0GB
	DAMO	190.00	160.00	75.00	145.00	148.30	164.41	157.50	155.75	131.50	110.00	1437.46	16.1GB

Table 2: Experimental results of various decoding strategies on MME dataset across three models: LLaVA1.5, INF-MLLM1 and mPLUG-Owl2.

Evaluation on Object Hallucination Dataset

▷ *Implementation* To evaluate the effectiveness of our method in addressing object hallucinations, we compared with various decoding strategies on the SEEM-annotated MSCOCO and A-OKVQA datasets provided by POPE. We reported four key metrics: Accuracy, Precision, Recall and F1 Score, focusing primarily on Accuracy and F1 Score for brevity, with complete results available in the Appendix.

Dataset			MSCOCO		A-OKVQA	
Setting	Model	Decoding	Accuracy	F1 Score	Accuracy	F1 Score
Random	LLaVA1.5	Regular	89.63	89.74	87.30	88.49
		VCD	87.53	87.81	85.00	86.49
		DOLA	89.67	89.74	87.40	88.57
		OPERA	89.87	89.95	87.27	88.50
		DAMO	89.97	89.92	87.90	88.93
	INF-MLLM1	Regular	91.17	90.92	90.60	90.97
		VCD	90.00	89.65	89.87	90.21
		DOLA	91.17	90.92	90.60	90.97
		OPERA	91.27	91.02	90.57	90.94
		DAMO	91.33	91.00	91.33	91.59
	mPLUG-Owl2	Regular	86.27	86.88	81.57	83.89
		VCD	84.40	84.79	82.53	84.16
		DOLA	86.33	86.92	81.83	84.07
		OPERA	86.23	86.84	81.53	83.86
		DAMO	87.20	87.44	84.60	86.03
	LLaVA1.5	Regular	86.23	86.82	80.30	83.21
		VCD	84.43	85.20	77.50	81.07
		DOLA	86.20	86.75	80.47	83.32
		OPERA	86.30	86.88	80.47	83.38
		DAMO	86.70	87.07	81.27	83.84
	INF-MLLM1	Regular	88.83	88.78	85.70	86.88
		VCD	87.60	87.43	85.00	86.17
		DOLA	88.83	88.78	85.70	86.88
		OPERA	88.80	88.74	85.70	86.89
		DAMO	89.30	89.11	86.67	87.62
	mPLUG-Owl2	Regular	80.73	82.52	75.97	79.98
		VCD	81.00	81.12	75.70	79.21
		DOLA	80.87	82.60	76.13	80.07
		OPERA	80.70	82.48	75.93	79.94
		DAMO	82.77	83.80	79.27	82.05
Popular	LLaVA1.5	Regular	79.70	81.71	69.33	76.10
		VCD	78.13	80.38	67.90	75.01
		DOLA	79.73	81.68	69.53	76.21
		OPERA	79.77	81.77	69.20	76.09
		DAMO	80.43	82.07	70.77	76.88
	INF-MLLM1	Regular	84.87	85.38	76.13	79.88
		VCD	84.17	84.47	76.37	79.82
		DOLA	84.87	85.38	76.13	79.88
		OPERA	84.87	85.36	76.10	79.85
		DAMO	85.73	86.00	77.43	80.71
	mPLUG-Owl2	Regular	76.17	77.69	67.37	74.63
		VCD	77.10	77.00	68.80	74.85
		DOLA	76.73	77.87	67.50	74.68
		OPERA	76.87	78.01	67.30	74.58
		DAMO	78.63	78.87	70.03	75.98
Adversarial	LLaVA1.5	Regular	79.70	81.71	69.33	76.10
		VCD	78.13	80.38	67.90	75.01
		DOLA	79.73	81.68	69.53	76.21
		OPERA	79.77	81.77	69.20	76.09
		DAMO	80.43	82.07	70.77	76.88
	INF-MLLM1	Regular	84.87	85.38	76.13	79.88
		VCD	84.17	84.47	76.37	79.82
		DOLA	84.87	85.38	76.13	79.88
		OPERA	84.87	85.36	76.10	79.85
		DAMO	85.73	86.00	77.43	80.71
	mPLUG-Owl2	Regular	76.17	77.69	67.37	74.63
		VCD	77.10	77.00	68.80	74.85
		DOLA	76.73	77.87	67.50	74.68
		OPERA	76.87	78.01	67.30	74.58
		DAMO	78.63	78.87	70.03	75.98

Table 3: Experimental results of various decoding strategies on the SEEM-annotated MSCOCO and A-OKVQA datasets from POPE using three models: LLaVA1.5, INF-MLLM1, and mPLUG-Owl2. The best values for each metric across all models and decoding strategies are highlighted in **bold**.

▷ *Q*: Does our proposed DAMO address object hallucinations effectively? Yes, DAMO achieves significant performance improvements in both accuracy and F1 score, as evidenced by results from MSCOCO and A-OKVQA datasets.

① *MSCOCO dataset* Results from the MSCOCO dataset, as shown in Table 3, demonstrated the effectiveness of DAMO. In the popular setting with mPLUG-Owl2, DAMO improved accuracy from 80.73% to 82.77%, while F1 score increased from 82.52% to 83.80%. In the challenging adversarial setting, DAMO further enhanced accuracy and F1 score on LLaVA1.5 compared to Regular decoding, with improvements of 0.73% and 0.36%, respectively. In contrast, methods like VCD sometimes exhibited performance declines; for instance, in the popular setting, VCD’s accuracy and F1 score dropped by 1.80% and 1.62% on LLaVA1.5 compared to Regular. The consistent superiority of DAMO reinforces the advantages of our approach.

② *A-OKVQA dataset* Turning to the A-OKVQA dataset shown in Table 3, DAMO again outperformed other decoding strategies. In the popular setting with mPLUG-Owl2, DAMO achieved significant improvements over the Regular decoding, with accuracy and F1 score increases of 3.30% and 2.07%, respectively, while other methods showed only minimal enhancements, with DOLA achieving improvements of merely 0.16% and 0.09%. The improvements on A-OKVQA were even more pronounced than those observed on MSCOCO, further underscoring the capability of our model.

Evaluation on Generalized Dataset

▷ *Implementation* To extend our evaluation beyond binary tasks, we conducted experiments on the generalized LLaVA-Bench dataset on LLaVA1.5, employing GPT-API for performance assessment, with the evaluation prompts detailed in the Appendix B.

▷ *Q: Can our proposed DAMO perform well on generalized dataset?* Yes, our DAMO demonstrated strong performance on the generalized LLaVA-Bench dataset. As shown in Table 4, our DAMO outperformed most decoding strategies across all categories. In the detailed description category, DAMO achieved a score of 75.87, surpassing DOLA by 1.20 points. It also excelled in complex reasoning, with a score of 88.39, which is significantly higher than OPERA’s 69.64. With an overall score of 78.13, our DAMO demonstrated enhanced robustness and generalizability across diverse tasks, suggesting its potential for solving other challenges as well.

Decoding	Conversation	Detail	Complex	Overall
Regular	58.82	70.33	87.79	75.22
VCD	60.88	59.67	83.46	71.12
DOLA	61.47	74.67	88.04	77.17
OPERA	66.76	51.00	69.64	64.17
DAMO	63.24	75.87	88.39	78.13

Table 4: Comparisons about various decoding methods on LLaVA1.5 using LLaVA-Bench dataset.

Evaluation about Adaptive Activation Refinement

▷ *Implementation* To fairly compare the effectiveness of adaptive starting layer selection strategies for activations refinement, we conducted several ablation experiments with fixed starting layers at the 0-th, 10-th, 16-th, 20-th, 24-th, and 28-th layers. All other parameters were kept consistent across experiments to ensure a fair comparison.

▷ *Q: Is our Adaptive Activation Refinement superior to the fixed layer starting for momentum?* Yes, the results presented in Figure 2a, obtained on the MME dataset with the LLaVA1.5 model, indicate that while fixed starting layers provide modest improvements over regular decoding, the adaptive layer selection consistently outperforms all fixed-layer approaches, demonstrating clear advantages by enabling a more responsive and effective decoding process.

Evaluation about Adaptive Coefficient Adjustment

▷ *Implementation* After determining the hallucination surge via adaptive activation refinement, we compared the performance of three setups: using only β_1 , using only β_2 (without switching), and employing the adaptive switching strategy between β_1 and β_2 . The experiments were conducted on the MME dataset using three models: LLaVA1.5, INF-MLLM1, and mPLUG-Owl2, with all other parameters kept constant across experiments.

▷ *Q: Does the adaptive momentum coefficient adjustment strategy outperform fixed coefficient setups?* Yes, the results presented in Figure 2b demonstrate that the adaptive β switching strategy con-

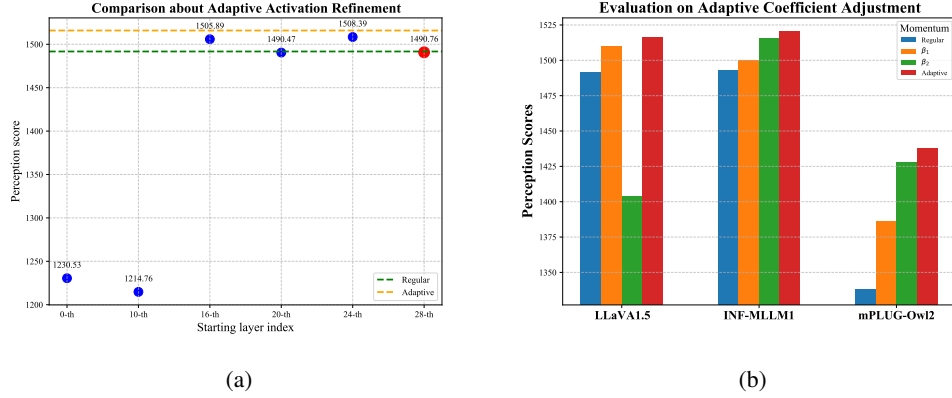


Figure 2: (a) Comparison of different starting layers for DAMO (0-th, 10-th, 16-th, 20-th, 24-th, and 28-th) against regular decoding and our adaptive activation refinement on the MME dataset using the LLaVA1.5 model. (b) Comparison results on adaptive momentum coefficient adjustment across LLaVA1.5, INF-MLLM1 and mPLUG-Owl2 on MME dataset. β_1 indicates the use of only β_1 , β_2 denotes the use on only β_2 , and *Adaptive* refers to adaptive adjustment between β_1 and β_2 .

sistently outperformed the fixed-coefficient setups across all models. For instance, in the mPLUG-Owl2 model, using β_1 resulted in a total score increase of 48.66, while β_2 provided a larger increase of 90.49. In contrast, our adaptive approach achieved an impressive total score improvement of 99.8.

Transferability Evaluation

▷ *Implementation* To evaluate DAMO’s transferability, we implemented it on the LLaMA2-7B model specifically targeting the effectiveness in addressing hallucinations in LLMs. The experiments focused on four datasets: TrthfulQA, FACTOR (News, Wiki), StrQA and GSM8K. We utilized Regular and DOLA decoding as baselines.

▷ *Q: Does our DAMO perform well when transferred to LLMs?* Yes, as shown in Table 5, DAMO improved performance on LLMs. In the TruthfulQA dataset, it outperformed Regular decoding in MC1 with a score of 34.15, surpassing both Regular (33.66) and DOLA (33.29). DAMO also excelled in the FACTOR task, scoring 57.48 on Wiki, higher than DOLA’s 56.51. These results demonstrate DAMO’s effectiveness when applied to LLMs, consistently improving performance across various language tasks.

Decoding	TruthfulQA (MC)			FACTOR		CoT	
	MC1	MC2	MC3	News	Wiki	StrQA	GSM8K
Regular	33.66	51.29	24.91	65.44	56.91	63.67	21.25
DOLA	33.29	60.84	29.79	61.58	56.51	64.59	21.83
DAMO	34.15	51.24	24.95	64.67	57.48	63.67	21.30

Table 5: Performance comparison of different decoding methods, including our transferred momentum decoding, applied to the LLaMA2-7B model across various language tasks.

5 CONCLUSION

We introduced DAMO, a momentum decoding method aimed at mitigating hallucinations in Vision-Language Models (LVLMs) by accumulating visual information from earlier layers. By refining the activations throughout the inference process, DAMO effectively preserves essential visual semantics, leading to more accurate and reliable predictions. Our method achieved excellent results on the MME, POPE, and LLaVA Bench datasets. Furthermore, we successfully transferred DAMO to LLaMA2, where it also demonstrated strong performance. These findings validate the effectiveness of our approach in enhancing model reliability across various tasks.

REFERENCES

- Vedika Agarwal, Rakshith Shetty, and Mario Fritz. Towards causal vqa: Revealing and reducing spurious correlations by invariant and covariant semantic editing. In *Proceedings of the IEEE/CVF Conference on Computer Vision and Pattern Recognition*, pp. 9690–9698, 2020.
- Aishwarya Agrawal, Dhruv Batra, and Devi Parikh. Analyzing the behavior of visual question answering models. *arXiv preprint arXiv:1606.07356*, 2016.
- Kwangjun Ahn, Xiang Cheng, Hadi Daneshmand, and Suvrit Sra. Transformers learn to implement preconditioned gradient descent for in-context learning. *Advances in Neural Information Processing Systems*, 36, 2024.
- Wenbin An, Feng Tian, Sicong Leng, Jiahao Nie, Haonan Lin, QianYing Wang, Guang Dai, Ping Chen, and Shijian Lu. Agla: Mitigating object hallucinations in large vision-language models with assembly of global and local attention. *arXiv preprint arXiv:2406.12718*, 2024.
- Ali Furkan Biten, Lluís Gómez, and Dimosthenis Karatzas. Let there be a clock on the beach: Reducing object hallucination in image captioning. In *Proceedings of the IEEE/CVF Winter Conference on Applications of Computer Vision*, pp. 1381–1390, 2022.
- Beitao Chen, Xinyu Lyu, Lianli Gao, Jingkuan Song, and Heng Tao Shen. Alleviating hallucinations in large vision-language models through hallucination-induced optimization. *arXiv preprint arXiv:2405.15356*, 2024a.
- Long Chen, Oleg Sinavski, Jan Hünemann, Alice Karnsund, Andrew James Willmott, Danny Birch, Daniel Maund, and Jamie Shotton. Driving with llms: Fusing object-level vector modality for explainable autonomous driving. In *2024 IEEE International Conference on Robotics and Automation (ICRA)*, pp. 14093–14100. IEEE, 2024b.
- Yen-Chun Chen, Linjie Li, Licheng Yu, Ahmed El Kholy, Faisal Ahmed, Zhe Gan, Yu Cheng, and Jingjing Liu. Uniter: Learning universal image-text representations.(2019). *arXiv preprint arXiv:1909.11740*, 2019.
- Yung-Sung Chuang, Yujia Xie, Hongyin Luo, Yoon Kim, James Glass, and Pengcheng He. Dola: Decoding by contrasting layers improves factuality in large language models. *arXiv preprint arXiv:2309.03883*, 2023.
- Karl Cobbe, Vineet Kosaraju, Mohammad Bavarian, Mark Chen, Heewoo Jun, Lukasz Kaiser, Matthias Plappert, Jerry Tworek, Jacob Hilton, Reiichiro Nakano, et al. Training verifiers to solve math word problems. *arXiv preprint arXiv:2110.14168*, 2021.
- Wenliang Dai, Junnan Li, Dongxu Li, Anthony Meng Huat Tiong, Junqi Zhao, Weisheng Wang, Boyang Li, Pascale Fung, and Steven Hoi. Instructblip: Towards general-purpose vision-language models with instruction tuning, 2023.
- Nicola De Cao, Wilker Aziz, and Ivan Titov. Editing factual knowledge in language models. *arXiv preprint arXiv:2104.08164*, 2021.
- Jacob Devlin. Bert: Pre-training of deep bidirectional transformers for language understanding. *arXiv preprint arXiv:1810.04805*, 2018.
- Maha Elbayad, Jiatao Gu, Edouard Grave, and Michael Auli. Depth-adaptive transformer. *arXiv preprint arXiv:1910.10073*, 2019.
- Chaoyou Fu, Peixian Chen, Yunhang Shen, Yulei Qin, Mengdan Zhang, Xu Lin, Jinrui Yang, Xiawu Zheng, Ke Li, Xing Sun, et al. Mme: A comprehensive evaluation benchmark for multimodal large language models. *arXiv preprint arXiv:2306.13394*, 2023.
- Anisha Gunjal, Jihan Yin, and Erhan Bas. Detecting and preventing hallucinations in large vision language models. In *Proceedings of the AAAI Conference on Artificial Intelligence*, volume 38, pp. 18135–18143, 2024.

- Mingzhe Hu, Shaoyan Pan, Yuheng Li, and Xiaofeng Yang. Advancing medical imaging with language models: A journey from n-grams to chatgpt. *arXiv preprint arXiv:2304.04920*, 2023.
- Qidong Huang, Xiaoyi Dong, Pan Zhang, Bin Wang, Conghui He, Jiaqi Wang, Dahua Lin, Weiming Zhang, and Nenghai Yu. Opera: Alleviating hallucination in multi-modal large language models via over-trust penalty and retrospection-allocation. In *Proceedings of the IEEE/CVF Conference on Computer Vision and Pattern Recognition*, pp. 13418–13427, 2024.
- Ziwei Ji, Nayeon Lee, Rita Frieske, Tiezheng Yu, Dan Su, Yan Xu, Etsuko Ishii, Ye Jin Bang, Andrea Madotto, and Pascale Fung. Survey of hallucination in natural language generation. *ACM Computing Surveys*, 55(12):1–38, 2023.
- Chao Jia, Yinfei Yang, Ye Xia, Yi-Ting Chen, Zarana Parekh, Hieu Pham, Quoc Le, Yun-Hsuan Sung, Zhen Li, and Tom Duerig. Scaling up visual and vision-language representation learning with noisy text supervision. In *International conference on machine learning*, pp. 4904–4916. PMLR, 2021.
- Jae Myung Kim, A Koepke, Cordelia Schmid, and Zeynep Akata. Exposing and mitigating spurious correlations for cross-modal retrieval. In *Proceedings of the IEEE/CVF Conference on Computer Vision and Pattern Recognition*, pp. 2585–2595, 2023.
- Jusung Lee, Sungguk Cha, Younghyun Lee, and Cheoljong Yang. Visual question answering instruction: Unlocking multimodal large language model to domain-specific visual multitasks. *arXiv preprint arXiv:2402.08360*, 2024.
- Sicong Leng, Hang Zhang, Guanzheng Chen, Xin Li, Shijian Lu, Chunyan Miao, and Lidong Bing. Mitigating object hallucinations in large vision-language models through visual contrastive decoding. In *Proceedings of the IEEE/CVF Conference on Computer Vision and Pattern Recognition*, pp. 13872–13882, 2024.
- Junnan Li, Dongxu Li, Silvio Savarese, and Steven Hoi. Blip-2: Bootstrapping language-image pre-training with frozen image encoders and large language models. In *International conference on machine learning*, pp. 19730–19742. PMLR, 2023a.
- Junnan Li, Dongxu Li, Silvio Savarese, and Steven Hoi. Blip-2: Bootstrapping language-image pre-training with frozen image encoders and large language models. In *International conference on machine learning*, pp. 19730–19742. PMLR, 2023b.
- Yifan Li, Yifan Du, Kun Zhou, Jinpeng Wang, Wayne Xin Zhao, and Ji-Rong Wen. Evaluating object hallucination in large vision-language models. *arXiv preprint arXiv:2305.10355*, 2023c.
- Stephanie Lin, Jacob Hilton, and Owain Evans. Truthfulqa: Measuring how models mimic human falsehoods. *arXiv preprint arXiv:2109.07958*, 2021.
- Tsung-Yi Lin, Michael Maire, Serge Belongie, James Hays, Pietro Perona, Deva Ramanan, Piotr Dollár, and C Lawrence Zitnick. Microsoft coco: Common objects in context. In *Computer Vision—ECCV 2014: 13th European Conference, Zurich, Switzerland, September 6-12, 2014, Proceedings, Part V 13*, pp. 740–755. Springer, 2014.
- Fang Liu, Yang Liu, Lin Shi, Houkun Huang, Ruifeng Wang, Zhen Yang, and Li Zhang. Exploring and evaluating hallucinations in llm-powered code generation. *arXiv preprint arXiv:2404.00971*, 2024a.
- Fuxiao Liu, Kevin Lin, Linjie Li, Jianfeng Wang, Yaser Yacoob, and Lijuan Wang. Aligning large multi-modal model with robust instruction tuning. *arXiv preprint arXiv:2306.14565*, 2023a.
- Haokun Liu, Yaonan Zhu, Kenji Kato, Izumi Kondo, Tadayoshi Aoyama, and Yasuhisa Hasegawa. Llm-based human-robot collaboration framework for manipulation tasks. *arXiv preprint arXiv:2308.14972*, 2023b.
- Haotian Liu, Chunyuan Li, Yuheng Li, and Yong Jae Lee. Improved baselines with visual instruction tuning, 2023c.

- Haotian Liu, Chunyuan Li, Yuheng Li, Bo Li, Yuanhan Zhang, Sheng Shen, and Yong Jae Lee. Llava-next: Improved reasoning, ocr, and world knowledge, January 2024b. URL <https://llava-vl.github.io/blog/2024-01-30-llava-next/>.
- Haotian Liu, Chunyuan Li, Qingyang Wu, and Yong Jae Lee. Visual instruction tuning. *Advances in neural information processing systems*, 36, 2024c.
- Haotian Liu, Chunyuan Li, Qingyang Wu, and Yong Jae Lee. Visual instruction tuning. *Advances in neural information processing systems*, 36, 2024d.
- Jiasen Lu, Dhruv Batra, Devi Parikh, and Stefan Lee. Vilbert: Pretraining task-agnostic vision-and-language representations for vision-and-language tasks. *Advances in neural information processing systems*, 32, 2019.
- Kevin Meng, David Bau, Alex Andonian, and Yonatan Belinkov. Locating and editing factual associations in gpt. *Advances in Neural Information Processing Systems*, 35:17359–17372, 2022.
- Dor Muhlgay, Ori Ram, Inbal Magar, Yoav Levine, Nir Ratner, Yonatan Belinkov, Omri Abend, Kevin Leyton-Brown, Amnon Shashua, and Yoav Shoham. Generating benchmarks for factuality evaluation of language models. *arXiv preprint arXiv:2307.06908*, 2023.
- Boris T Polyak. Some methods of speeding up the convergence of iteration methods. *Ussr computational mathematics and mathematical physics*, 4(5):1–17, 1964.
- Alec Radford, Jong Wook Kim, Chris Hallacy, Aditya Ramesh, Gabriel Goh, Sandhini Agarwal, Girish Sastry, Amanda Askell, Pamela Mishkin, Jack Clark, et al. Learning transferable visual models from natural language supervision. In *International conference on machine learning*, pp. 8748–8763. PMLR, 2021.
- Tal Schuster, Adam Fisch, Jai Gupta, Mostafa Dehghani, Dara Bahri, Vinh Tran, Yi Tay, and Donald Metzler. Confident adaptive language modeling. *Advances in Neural Information Processing Systems*, 35:17456–17472, 2022.
- Dustin Schwenk, Apoorv Khandelwal, Christopher Clark, Kenneth Marino, and Roozbeh Mottaghi. A-okvqa: A benchmark for visual question answering using world knowledge. In *European conference on computer vision*, pp. 146–162. Springer, 2022.
- Ilya Sutskever, James Martens, George Dahl, and Geoffrey Hinton. On the importance of initialization and momentum in deep learning. In *International conference on machine learning*, pp. 1139–1147. PMLR, 2013.
- Hao Tan and Mohit Bansal. Lxmert: Learning cross-modality encoder representations from transformers. *arXiv preprint arXiv:1908.07490*, 2019.
- Surat Teerapittayanon, Bradley McDanel, and Hsiang-Tsung Kung. Branchynet: Fast inference via early exiting from deep neural networks. In *2016 23rd international conference on pattern recognition (ICPR)*, pp. 2464–2469. IEEE, 2016.
- Lei Wang, Jiabang He, Shenshen Li, Ning Liu, and Ee-Peng Lim. Mitigating fine-grained hallucination by fine-tuning large vision-language models with caption rewrites. In *International Conference on Multimedia Modeling*, pp. 32–45. Springer, 2024.
- Ziwei Xu, Sanjay Jain, and Mohan Kankanhalli. Hallucination is inevitable: An innate limitation of large language models. *arXiv preprint arXiv:2401.11817*, 2024.
- Jia-Yu Yao, Kun-Peng Ning, Zhen-Hui Liu, Mu-Nan Ning, and Li Yuan. Llm lies: Hallucinations are not bugs, but features as adversarial examples. *arXiv preprint arXiv:2310.01469*, 2023.
- Qinghao Ye, Haiyang Xu, Guohai Xu, Jiabo Ye, Ming Yan, Yiyang Zhou, Junyang Wang, Anwen Hu, Pengcheng Shi, Yaya Shi, et al. mplug-owl: Modularization empowers large language models with multimodality. *arXiv preprint arXiv:2304.14178*, 2023a.
- Qinghao Ye, Haiyang Xu, Jiabo Ye, Ming Yan, Anwen Hu, Haowei Liu, Qi Qian, Ji Zhang, Fei Huang, and Jingren Zhou. mplug-owl2: Revolutionizing multi-modal large language model with modality collaboration, 2023b.

- Shukang Yin, Chaoyou Fu, Sirui Zhao, Tong Xu, Hao Wang, Dianbo Sui, Yunhang Shen, Ke Li, Xing Sun, and Enhong Chen. Woodpecker: Hallucination correction for multimodal large language models. *arXiv preprint arXiv:2310.16045*, 2023.
- Yan Zeng, Xinsong Zhang, and Hang Li. Multi-grained vision language pre-training: Aligning texts with visual concepts. *arXiv preprint arXiv:2111.08276*, 2021.
- Muru Zhang, Ofir Press, William Merrill, Alisa Liu, and Noah A Smith. How language model hallucinations can snowball. *arXiv preprint arXiv:2305.13534*, 2023a.
- Yue Zhang, Yafu Li, Leyang Cui, Deng Cai, Lemao Liu, Tingchen Fu, Xinting Huang, Enbo Zhao, Yu Zhang, Yulong Chen, et al. Siren’s song in the ai ocean: a survey on hallucination in large language models. *arXiv preprint arXiv:2309.01219*, 2023b.
- Qiang Zhou, Zhibin Wang, Wei Chu, Yinghui Xu, Hao Li, and Yuan Qi. Infmlm: A unified framework for visual-language tasks, 2023a.
- Yiyang Zhou, Chenhang Cui, Jaehong Yoon, Linjun Zhang, Zhun Deng, Chelsea Finn, Mohit Bansal, and Huaxiu Yao. Analyzing and mitigating object hallucination in large vision-language models. *arXiv preprint arXiv:2310.00754*, 2023b.
- Deyao Zhu, Jun Chen, Xiaoqian Shen, Xiang Li, and Mohamed Elhoseiny. Minigpt-4: Enhancing vision-language understanding with advanced large language models. *arXiv preprint arXiv:2304.10592*, 2023a.
- Deyao Zhu, Jun Chen, Xiaoqian Shen, Xiang Li, and Mohamed Elhoseiny. Minigpt-4: Enhancing vision-language understanding with advanced large language models. *arXiv preprint arXiv:2304.10592*, 2023b.
- Deyao Zhu, Jun Chen, Xiaoqian Shen, Xiang Li, and Mohamed Elhoseiny. Minigpt-4: Enhancing vision-language understanding with advanced large language models. *arXiv preprint arXiv:2304.10592*, 2023c.
- Jiawei Zhu, Yishu Liu, Huanjia Zhu, Hui Lin, Yuncheng Jiang, Zheng Zhang, and Bingzhi Chen. Combating visual question answering hallucinations via robust multi-space co-debias learning. In *ACM Multimedia 2024*, 2024a.
- Lanyun Zhu, Deyi Ji, Tianrun Chen, Peng Xu, Jieping Ye, and Jun Liu. Ibd: Alleviating hallucinations in large vision-language models via image-biased decoding. *arXiv preprint arXiv:2402.18476*, 2024b.

A DETAILED RESULTS

We present the detailed results corresponding to Figure 2a and 2b, which are elaborated in Table 6 and Table 7, respectively.

Layer Selection	Existence	Count	Position	Color	Posters	Celebrity	Scene	Landmark	Artwork	OCR	Total
Regular	190.00	160.00	138.33	165.00	141.50	135.88	156.25	161.25	118.50	125.00	1491.71
0-th	185.00	115.00	123.33	153.33	78.57	90.29	139.75	107.00	105.75	132.5	1230.53
10-th	185.00	115.00	118.33	168.33	81.63	89.71	136.00	102.75	108.00	110.00	1214.76
16-th	195.00	145.00	138.33	165.00	143.54	136.76	157.75	166.00	118.50	140.00	1505.89
20-th	195.00	150.00	133.33	165.00	142.52	134.12	157.00	165.25	115.75	132.50	1490.47
24-th	195.00	153.33	148.33	165.00	142.52	134.71	157.00	163.75	116.25	132.50	1508.39
28-th	195.00	148.33	143.33	160.00	142.52	133.82	157.00	163.75	114.50	132.50	1490.76
Adaptive	195.00	150.00	143.33	165.00	144.56	135.00	157.00	166.00	120.00	140.00	1515.89

Table 6: Comparison of different momentum decoding starting layers (0-th, 10-th, 16-th, 20-th, 24-th, and 28-th) against regular decoding and our adaptive layer selection on the MME dataset using the LLaVA 1.5 model.

Model	Decoding	Existence	Count	Position	Color	Posters	Celebrity	Scene	Landmark	Artwork	OCR	Total
LLaVA 1.5	Regular	190.00	160.00	138.33	165.00	141.50	135.88	156.25	161.25	118.50	125.00	1491.71
	β_1	195.00	156.67	148.33	170.00	136.39	132.65	155.50	158.25	117.00	140.00	1509.79
	β_2	190.00	120.00	145.00	175.00	122.45	120.00	145.25	136.00	110.25	140.00	1403.95
	Adaptive	195.00	150.00	143.33	165.00	144.56	135.00	157.00	166.00	120.00	140.00	1515.89
INF-MLLM	Regular	195.00	150.00	151.67	160.00	150.00	140.29	157.75	155.50	122.50	110.00	1492.71
	β_1	195.00	145.00	151.67	165.00	148.64	145.59	156.75	150.75	124.00	117.50	1499.89
	β_2	190.00	150.00	151.67	165.00	149.66	148.53	155.50	151.25	129.00	125.00	1515.61
	Adaptive	195.00	150.00	158.33	165.00	148.64	146.76	156.25	154.75	128.50	117.50	1520.74
mPLUG-Owl2	Regular	180.00	145.00	73.33	136.67	136.73	141.18	157.25	137.75	127.25	102.50	1337.66
	β_1	180.00	160.00	73.33	153.33	131.97	151.18	157.75	136.00	132.75	110.00	1386.32
	β_2	185.00	160.00	71.67	155.00	144.90	160.59	157.50	151.25	132.25	110.00	1428.15
	Adaptive	190.00	160.00	75.00	145.00	148.30	164.41	157.50	155.75	131.50	110.00	1437.46

Table 7: Comparison results on adaptive momentum coefficient adjustment across LLaVA1.5, INF-MLLM1 and mPLUG-Owl2 on MME dataset. β_1 indicates the use of only β_1 , β_2 denotes the use on only β_2 , and *Adaptive* refers to adaptive switching between β_1 and β_2 .

B PROMPT

We present the prompt used in Table 4, which is used to evaluate the model’s responses generated on the LLaVA-Bench dataset.

You are an evaluator for Visual Question Answering (VQA) tasks. Your goal is to score the generated answer based on its relevance and accuracy compared to the ground truth annotations. Follow these instructions carefully:

1. ****Understand the Question****: Identify what is being asked and the context provided by the ground truth annotations.
2. ****Evaluate the Generated Answer****: Compare the generated answer with the ground truth annotations. Consider its accuracy, relevance, and completeness.
3. ****Provide a Score****: Assign a score between 0 and 100, where 0 indicates no relevance and 100 indicates a perfect match.
4. ****You should be a restrict evaluator. And you just need to output a score, any explanations are not allowed**

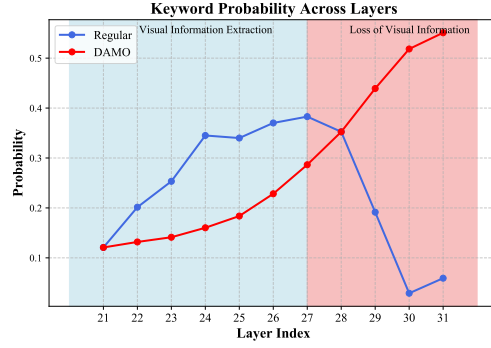
Inputs:

- Question: {replace with your question}
- Ground Truth Image Annotations: {ground_truth_annotations provided by LLaVA-Bench}
- Generated Answer: {replace with your answer}

Your Score (0-100):

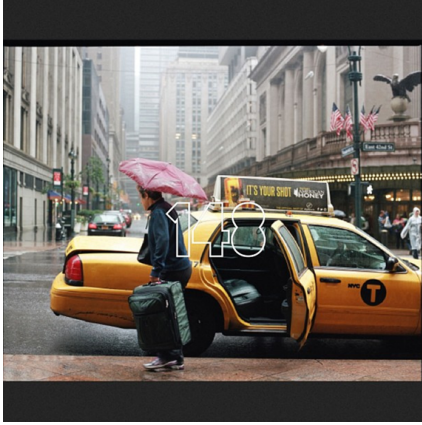


(a) The image input.

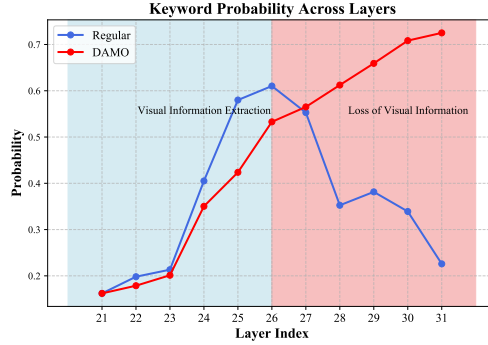


(b) The probability of key words across layers.

Figure 3: Instance 1 for our motivation.



(a) The image input.



(b) The probability of key words across layers.

Figure 4: Instance 2 for our motivation.

C SOME INSTANCES RELEVANT TO FIGURE 1B.

We present more 2 instances here generated from MiniGPT-4. Similar to Figure 1b, the blue curve represents the Regular Decoding, and the red one denotes our DAMO.

Instance 1: Given the question “How many plates are in this image?” and the image shown in Figure 3a, the probability of correct word ‘two’ varies across layers, which is shown in Figure 3b.

Instance 2: Given the question “What color is the taxi in this image?” and the image shown in Figure 4a, the probability of correct word ‘yellow’ varies across layers, which is shown in Figure 4b.

D HYPERPARAMETER SETTING

We provide our detailed hyperparameter setting in Table 8. α is set to 0.7 for all experiments. And we present different hyperparameters including τ , β_1 and β_2 for different tasks across different models. M represents MME dataset and P denotes POPE dataset.

	LLaVA M	LLaVA P	INF M	INF P	mPLUG M	mPLUG P
β_1	0.05	0.20	0.20	0.05	0.60	0.40
β_2	0.20	0.40	0.40	0.10	0.80	0.60
τ	-0.30	-0.30	-0.60	-0.60	-0.30	-0.30

Table 8: Hyperparameters for different tasks across different models

E MORE ABLATION STUDIES

E.1 EVALUATING THE SENSITIVITY OF DIFFERENT τ

We evaluate the sensitivity of different τ on POPE (MSCOCO setting) dataset using LLaVA1.5 model and report F1 score. As shown in Table 9, by setting τ to 0.3, 0, -0.3, and -0.6, we observe that the model’s performance varies accordingly. This demonstrates the model’s sensitivity to τ . Notably, when τ is set to our default value of 0.3, the model achieves its best performance.

τ	0.3	0	-0.3	-0.6
Random	88.83	89.56	89.92	89.62
Popular	86.60	86.43	87.07	86.66
Adversarial	81.95	81.56	82.07	81.78

Table 9: The sensitivity of τ on POPE (MSCOCO) dataset using LLaVA1.5 model.

E.2 EVALUATING THE SENSITIVITY OF DIFFERENT β_1

We evaluate different β_1 values to observe performance variations on the MME dataset using LLaVA1.5 model. For a fair comparison, β_2 is set to its default value of 0.2. In this experiment, we explore setting β_1 to 0.01, 0.05, 0.1, 0.15, and 0.2, and analyze the corresponding results.

As shown in Table 10, LLaVA1.5 is quite sensitive to the value of β_1 . When β_1 is set to smaller values, the model shows improved performance compared to the baseline. However, as β_1 increases to 0.20, a noticeable performance drop is observed. This highlights that 0.05 is the optimal parameter setting.

β_1	Existence	Count	Position	Color	Posters	Celebrity	Scene	Landmark	Artwork	OCR	Total
0.01	190.00	145.00	135.00	160.00	149.66	137.35	160.00	168.50	119.75	137.50	1502.76
0.05	195.00	150.00	143.33	165.00	144.56	135.00	157.00	166.00	120.00	140.00	1515.89
0.10	195.00	151.67	153.33	170.00	136.39	130.00	155.50	160.50	117.75	125.00	1495.14
0.15	190.00	153.33	143.33	180.00	125.51	122.94	151.00	150.75	113.00	132.50	1462.37
0.20	190.00	120.00	145.00	175.00	122.45	120.00	145.25	136.00	110.25	140.00	1403.95

Table 10: Comparison of different β_1 on the MME dataset using LLaVA1.5 model.

E.3 EVALUATING THE SENSITIVITY OF DIFFERENT β_2

Similar to the evaluation of β_1 , we fix β_1 at 0.05 and evaluate the performance across different β_2 values: 0.1, 0.2, 0.4, 0.6, and 0.8.

As shown in Table 11, the model’s performance is significantly affected by changes in β_2 . When β_2 is set too high, the model’s performance rapidly declines, as this interferes with the model’s normal reasoning process. Our experiments also confirm that the default setting of β_2 at 0.2 is optimal.

β_2	Existence	Count	Position	Color	Posters	Celebrity	Scene	Landmark	Artwork	OCR	Total
0.10	195.00	156.67	143.33	170.00	138.44	133.53	156.25	160.50	118.75	125.00	1497.46
0.20	195.00	150.00	143.33	165.00	144.56	135.00	157.00	166.00	120.00	140.00	1515.89
0.40	185.00	130.00	133.33	143.33	137.41	123.82	159.25	160.00	110.00	102.50	1384.66
0.60	188.33	103.33	93.33	120.00	123.81	107.94	132.75	124.00	88.25	105.00	1186.75
0.80	183.33	113.33	91.67	135.00	121.09	102.35	127.75	121.50	85.25	122.50	1203.77

Table 11: Comparison of different β_2 on the MME dataset using LLaVA1.5 model.

E.4 EVALUATING THE EFFECT OF OUR PROPOSED ADAPTIVE ACTIVATION REFINEMENT MECHANISM

In addition to testing the effectiveness of our adaptive activation refinement mechanism on LLaVA1.5, we further evaluate it on INF-MLLM1 by setting the starting layer to the 16th, 20th, 24th, and 28th layers.

	Existence	Count	Position	Color	Posters	Celebrity	Scene	Landmark	Artwork	OCR	Total
16-th	190.00	150.00	158.33	165.00	146.94	147.65	157.00	150.75	126.75	117.50	1509.92
20-th	190.00	150.00	158.33	165.00	145.92	147.65	156.25	150.00	128.50	125.00	1516.65
24-th	185.00	145.00	163.33	165.00	142.86	149.12	154.75	147.75	128.25	132.50	1513.56
28-th	190.00	140.00	158.33	165.00	143.88	148.82	154.75	147.00	127.25	132.50	1507.53
Adaptive	195.00	150.00	158.33	165.00	148.64	146.76	156.25	154.75	128.50	117.50	1520.74

Table 12: Comparison of different momentum decoding starting layers (16-th, 20-th, 24-th, and 28-th) against regular decoding and our adaptive layer selection on the MME dataset using the INF-MLLM1 model.

As shown in Table 12, our adaptive starting layer method outperforms all fixed starting layer settings, further demonstrating the effectiveness of our approach.

F TEXT QUALITY

F.1 TEXT GENERATED AT PRECEDING LAYERS

As shown in Figure 5, we present an example from Figure 1, showing the decoding results at different layers. The tokens with the highest probabilities are displayed for each layer, with the color intensity representing the token probabilities—darker colors indicate higher probabilities. As expected, the model consistently generates higher-quality text at the later layers, aligning with common understanding.

F.2 QUALITY OF OVERALL GENERATED TEXTS

For convenience, we used the GPT-API to evaluate the quality of the generated text from several perspectives: Fluency, Coherence, Grammar and Syntax, and Vocabulary Usage. Due to resource constraints, we randomly sampled 50 questions from the POPE dataset using LLaVA1.5. We then compared the average evaluation scores of text quality generated by Regular, VCD, DoLA, OPERA, and DAMO, as shown in the Table 13. We also present the GPT prompt used for the evaluation.

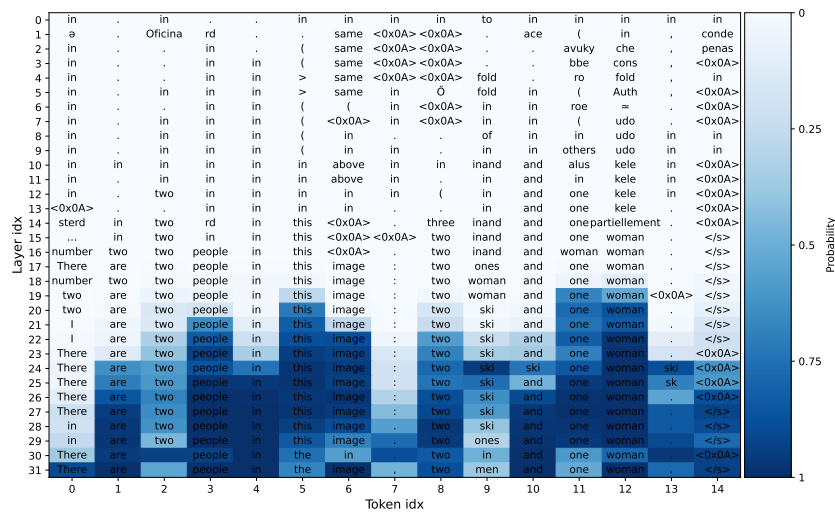


Figure 5: The decoding tokens across different layers from question illustrated in Figure 1.

“You are an expert linguist and writing coach. Carefully evaluate the following text generated by a language model based on the following criteria:

Fluency: Assess the smoothness of the text. Are the sentences well-constructed, and do they flow naturally?

Coherence: Determine whether the ideas are logically connected and easy to follow. Does the text maintain a consistent train of thought?

Grammar and Syntax: Check for grammatical accuracy and proper sentence structure.

Vocabulary Usage: Analyze the choice of words. Are they appropriate, diverse, and effectively used to convey meaning?

Relevance: Consider how well the text adheres to the given context or topic. Does it stay on point and address the subject effectively?

Creativity and Originality (optional): If applicable, evaluate the uniqueness and innovation in the text's ideas or phrasing.

Provide a comprehensive evaluation of the text, highlighting both strengths and areas for improvement. Conclude with an overall quality score out of 10, justifying your decision.”

Text to Evaluate: {answer}

Your Numerical Score (0-10):

Method	Regular	VCD	DoLA	OPERA	DAMO
Score	7.9	7.8	8.1	8.0	8.1

Table 13: Quality scores from different decoding methods for text generated by LLaVA1.5, evaluated across various criteria such as fluency, coherence, grammar and syntax, and vocabulary usage.

G COMPLEX REASONING

To further explore DAMO’s performance in complex reasoning, we present a case study as shown in Table 14. Given an animated image and the question “Are all the characters in this figure from The Story of the Little Mole?”, we compare the outputs from different decoding methods using LLaVA1.5 model and evaluate their scores using GPT.

As shown in Table 14, since the temperature was set to 0 for fair comparison, we observed that the answers generated by DoLA and OPERA were identical to those from Regular decoding. This indicates that these decoding methods are not sensitive to this particular problem and fail to effectively detect and mitigate hallucinations. While VCD produced a different answer, it did not adequately address the question. In contrast, only DAMO correctly identified that “Jerry the Mouse” is from the popular cartoon “Tom and Jerry” and not from “The Story of the Little Mole”, showcasing DAMO’s strength in complex reasoning tasks.


Input	Are all the characters in this figure from The Story of the Little Mole?		GPT-Evaluation
Regular	No, not all the characters in the figure are from The Story of the Little Mole. The figure includes a variety of characters, such as a mouse, a hedgehog, a frog, a turtle, and a rabbit, as well as a character from The Story of the Little Mole.	Score: 3/5 The answer is partially correct but lacks precision and explicit mention of the character from a different franchise.	
VCD	No, not all the characters in the figure are from The Story of the Little Mole. The characters include a mouse, a frog, a hedgehog, a mole, and a squirrel, but there is also a character from Paddington Bear.	Score: 2/5 The answer recognizes that not all characters are from The Story of the Little Mole, but it makes a significant factual error regarding the character from another series.	
DOLA	No, not all the characters in the figure are from The Story of the Little Mole. The figure includes a variety of characters, such as a mouse, a hedgehog, a frog, a turtle, and a rabbit, as well as a character from The Story of the Little Mole.	Score: 3/5 While the general idea is correct, the lack of specific identification of Jerry as the character from Tom and Jerry prevents this answer from being fully accurate and detailed.	
OPERA	No, not all the characters in the figure are from The Story of the Little Mole. The figure includes a variety of characters, such as a mouse, a hedgehog, a frog, a turtle, and a rabbit, as well as a character from The Story of the Little Mole.	Score: 3/5 The answer gets the general idea right but lacks the necessary precision in identifying Jerry as the character from a different cartoon series, which affects its overall clarity and completeness.	
DAMO	No, not all the characters in the figure are from The Story of the Little Mole. Jerry the Mouse is from the popular cartoon “Tom and Jerry,” and he is not from “The Story of the Little Mole.” The other characters in the figure are from ”The Story of the Little Mole.”	Score: 5/5 This answer is completely accurate and appropriately detailed, clearly identifying the outlier character and demonstrating full understanding of the question and the ground truth.	

Table 14: Comparison of complex reasoning generated by LLaVA1.5 using different decoding strategies for a given image and text along with evaluations and explanations from GPT-4.

H EVALUATION ON OTHER HALLUCINATION BENCHMARK

HallusionBench is a benchmark designed to evaluate hallucinations in large visual-language models (LVLMs). It consists of 346 images and 1,129 expert-crafted questions aimed at assessing models’ tendencies, logical consistency, and failure modes, particularly focusing on hallucinations and visual

illusions. Here we adopt HallusionBench to further evaluate our DAMO. The result is evaluated by GPT-API according to the official setting.

Model	Decoding	qAcc	fAcc	easy aAcc	hard aAcc	aAcc
LLaVA1.5	Regular	8.13	14.16	36.92	27.91	35.43
	VCD	9.01	14.16	36.70	29.53	35.96
	DoLA	9.45	14.45	36.70	29.07	36.23
	OPERA	8.57	14.45	37.14	29.07	35.96
	DAMO	9.67	14.74	37.14	29.77	36.58
INF-MLLM1	Regular	7.69	14.45	41.98	29.07	38.62
	VCD	7.25	13.01	40.66	28.37	37.73
	DoLA	7.03	13.01	40.22	29.30	38.00
	OPERA	7.25	13.87	41.76	27.44	37.91
	DAMO	8.13	14.16	42.42	29.77	38.97
mPLUG-Owl2	Regular	10.33	14.45	39.56	30.23	38.18
	VCD	10.55	15.61	36.92	30.23	38.80
	DoLA	10.33	14.74	39.56	30.47	38.44
	OPERA	9.23	14.45	39.78	28.37	38.26
	DAMO	10.77	15.90	40.00	30.70	39.06

Table 15: Performances on HallusionBench using different decoding methods across three models.

As shown in Table 15, DAMO performs exceptionally well on HallusionBench. Except for the INF-MLLM1 setting, where no decoding method outperforms regular decoding, DAMO consistently outperforms all other methods across all other settings. This demonstrates DAMO’s strong capability in addressing hallucination issues effectively.